Development and Evaluation of Airborne Multipath Error Bounds for L1-L5

Juan Blanch, Todd Walter, R. Eric Phelts

Stanford University

ABSTRACT

Current aviation standards define a multipath error model that is valid after the smoothing filter is assumed to have converged (assuming a 100 s Hatch filter). The draft standards for dual frequency Satellite-based Augmentation Systems further specify an error model when the code has not been smoothed, and it is defined as a multiple of the converged value. In this paper, multipath and noise error bounds are derived as a function of smoothing time assuming a first order model for the code multipath and the receiver noise. These error bounds are evaluated using GPS and Galileo measurements collected in flight. The derived model appears to account well for the error reduction as a function of smoothing time.

INTRODUCTION

The standards for Satellite-based Augmentation Systems (SBAS) Dual Frequency Multi-constellation (DFMC) are currently being developed. With dual frequency, the residual ionospheric delay error (which is the largest contributor in single frequency) is no longer the dominant term. In particular, multipath and receiver noise is now a much more important term in the error budget. For this reason, and because of the introduction of new signals (L5 and E5a), these term is receiving more attention, and new data suggests that extrapolating L1 models to L5 and L1-L5 combination might not be sufficient [5].

This multipath and antenna group delay error model used in single frequency SBAS has been in place since 2000 [1]. This model is elevation dependent and only applies once the carrier smoothing filter has converged, which is assumed to occur after 360 s of smoothing. The current standards do not specify how the multipath error bound varies with smoothing time before convergence. The draft SBAS DFMC Minimum Operational Standards [2] (developed within EUROCAE) specifies an additional constraint: for unsmoothed code measurements, the standard deviation is ten times higher than the value at convergence.

A strict application of this error model between t=0 and t = 360 s would result in very conservative error bounds, because in reality the actual errors decrease steadily as new measurements are added. In particular, it could result in significant performance losses in the presence of cycle slips. This is especially critical for environments with ionospheric scintillation (for example in low latitudes), where we expect a much higher cycle slip rate. And even if the receivers do use a less conservative multipath curve, service providers evaluating coverage would need to assume the minimum requirement, and therefore could be unable to claim availability where there might be.

The goal of this paper is twofold: to derive a multipath error model that is valid before convergence, and to evaluate it using GNSS airborne measurements. In the first part, we develop three models: one corresponding to time invariant smoothing, one corresponding to time varying smoothing, and one where we start with a time varying smoothing that switches to time invariant after a set time interval. In the second part, we evaluate the multipath error model using GNSS data collected in flight.

MULTIPATH ERROR MODEL AT CONVERGENCE

In this paper, we will assume that the error model at convergence is given by the formulas specified in [2], which are based on the ones used in [1]:

$$\sigma_{air} = \sqrt{\frac{f_{L1}^4 + f_{L5}^4}{\left(f_{L1}^2 - f_{L5}^2\right)^2}} \sqrt{\left(\sigma_{MP\&AGVD,i}\right)^2 + \left(\sigma_{noise,i}\right)^2} \tag{1}$$

Where:

$$\sigma_{MP}(\theta) = 0.13[\mathrm{m}] + 0.53[\mathrm{m}]\exp(-\theta/10[\mathrm{deg}]) \tag{2}$$

We will further assume that the temporal error model can be modeled as:

$$\sigma_{air}(k) = \sqrt{\frac{f_{L1}^4 + f_{L5}^4}{\left(f_{L1}^2 - f_{L5}^2\right)^2}} \sqrt{A_{MP}(k)\left(\sigma_{MP\&AGVD,i}\right)^2 + A_{noise}(k)\left(\sigma_{noise,i}\right)^2} \tag{3}$$

Where *k* is the time step, and A_{MP} are A_{noise} are functions such that:

$$\begin{aligned} &A_{MP}(0) = 100, \\ &A_{MP}(360) = 1, \\ &A_{noise}(0) = 200, \\ &A_{noise}(360) = 1 \end{aligned} \tag{4}$$

These values are based on the standards under development for dual frequency SBAS [2]. The purpose of the next section is to define the behavior of the convergence curve between t = 0 and 1 = 360 s.

TIME VARYING ERROR MODEL DERIVATION

Temporal model for normalized code multipath and normalized receiver noise

The formulas for the standard deviation are derived assuming that the code multipath follows a first order Gauss-Markov model, which is the simplest assumption (short of assuming independent samples):

$$\begin{aligned} &\eta_k = \alpha\eta_{k-1} + \theta_k \\ &\theta_k \sim N\left(0, \sqrt{1-\alpha^2}\right) \end{aligned} \tag{5}$$

where η_k is the code multipath noise at epoch *k* and α is the correlation between samples (we will assume a 1 Hz sampling rate). The process is such that we have:

$$\mathrm{cov}(\eta_k, \eta_l) = \alpha^{|k-l|} \tag{6}$$

Smoothing filter

The smoothing process typically has two sections, a time varying section followed by a time invariant one. For the time varying section we have:

$$\varepsilon_k = \left(1-\frac{1}{k}\right)\varepsilon_{k-1} + \frac{1}{k}\eta_k \tag{7}$$

In the time invariant section that follows, we have:

$$\varepsilon_k = \left(1-\frac{1}{K}\right)\varepsilon_{k-1} + \frac{1}{K}\eta_k \tag{8}$$

where *K* is the smoothing constant (in [1], it is set to 100 s).

Error variance for the time varying section

For $k \le K$, ε_k is the average of the first *k* measurements. We calculate the variance of the sum:

$$\sum_{i=1}^{k}\eta_i = k\varepsilon_k \tag{9}$$

We have:

$$\operatorname{cov}\left(\sum_{i=1}^{k}\eta_i\right) = \begin{bmatrix}1 & \cdots & 1\end{bmatrix}\begin{bmatrix}1 & \alpha & \cdots & \alpha^{k-1}\\ \alpha & \ddots & \ddots & \vdots\\ \vdots & \ddots & \ddots & \alpha\\ \alpha^{k-1} & \cdots & \alpha & 1\end{bmatrix}\begin{bmatrix}1\\ \vdots\\ 1\end{bmatrix} \tag{10}$$

We can further develop this expression:

$$\begin{aligned}\operatorname{cov}\left(\sum_{i=1}^{k}\eta_i\right) &= 2\sum_{i=0}^{k-1}\sum_{j=0}^{i}\alpha^j - k = 2\sum_{i=0}^{k-1}\frac{1-\alpha^{i+1}}{1-\alpha} - k\\ &= \frac{2k}{1-\alpha} - \frac{2\alpha}{1-\alpha}\sum_{i=0}^{k-1}\alpha^i - k = \frac{2k}{1-\alpha} - \frac{2\alpha}{(1-\alpha)^2}\left(1-\alpha^k\right) - k\\ &= k\frac{1+\alpha}{1-\alpha} - \frac{2\alpha}{(1-\alpha)^2}\left(1-\alpha^k\right)\end{aligned} \tag{11}$$

We have therefore for $k \le K$:

$$\operatorname{cov}\left(\varepsilon_k\right) = \frac{1+\alpha}{k(1-\alpha)} - \frac{2\alpha}{k^2(1-\alpha)^2}\left(1-\alpha^k\right) \tag{12}$$

Error variance in the time invariant section

For *k>K* we have:

$$\varepsilon_k = \left(1-\frac{1}{K}\right)^{k-K}\varepsilon_K + \frac{1}{K}\sum_{i=K+1}^{k}\left(1-\frac{1}{K}\right)^{k-i}\eta_i \tag{13}$$

We note:

$$A = 1 - \frac{1}{K}$$
$$v_k = \varepsilon_{k+K} \tag{14}$$

We have:

$$v_k = A^k \varepsilon_K + \frac{A^{k-1}}{K} \sum_{i=0}^{k-1} A^{-i} \eta_{K+i+1} \tag{15}$$

After some derivations, it can be shown that:

$$\begin{aligned}
&\operatorname{cov}\left(\sum_{i=0}^{k-1} A^{-i} \eta_{i+1} \right) = \sum_{i,j} A^{-i-j} \alpha^{|i-j|} = \sum_{i=0}^{k-1} A^{-2i} + 2 \sum_{i>j} A^{-i-j} \alpha^{i-j} \\
&= \sum_{i=0}^{k-1} A^{-2i} + 2 \sum_{j=0}^{k-1} (A\alpha)^{-j} \sum_{i=j+1}^{k-1} \left(\frac{\alpha}{A} \right)^i = \frac{1 - A^{-2k}}{1 - A^{-2}} + 2 \sum_{j=0}^{k-1} \frac{\alpha}{A} A^{-2j} \sum_{i=0}^{k-j-2} \left(\frac{\alpha}{A} \right)^i \\
&= \frac{1 - A^{-2k}}{1 - A^{-2}} + 2 \sum_{j=0}^{k-1} \frac{\alpha}{A} A^{-2j} \left(\frac{1 - \left(\frac{\alpha}{A} \right)^{k-j-1}}{1 - \frac{\alpha}{A}} \right) = \frac{1 - A^{-2k}}{1 - A^{-2}} + 2 \frac{\alpha}{A - \alpha} \sum_{j=0}^{k-1} A^{-2j} - 2 \frac{\alpha}{A - \alpha} \left(\frac{\alpha}{A} \right)^{k-1} \sum_{j=0}^{k-1} \left(\frac{1}{A\alpha} \right)^j \\
&= \frac{1 - A^{-2k}}{1 - A^{-2}} + 2 \frac{\alpha}{A - \alpha} \frac{1 - A^{-2k}}{1 - A^{-2}} - 2 \frac{\alpha}{A - \alpha} \left(\frac{\alpha}{A} \right)^{k-1} \frac{1 - (A\alpha)^{-k}}{1 - (A\alpha)^{-1}}
\end{aligned} \tag{16}$$

Therefore, we have:

$$\begin{aligned}
&\operatorname{cov}\left(\frac{A^{k-1}}{K} \sum_{i=0}^{k-1} A^{-i} \eta_{i+1} \right) = \frac{A^{2k-2}}{K^2} \left(\frac{1 - A^{-2k}}{1 - A^{-2}} + 2 \frac{\alpha}{A - \alpha} \frac{1 - A^{-2k}}{1 - A^{-2}} - 2 \frac{\alpha}{A - \alpha} \left(\frac{\alpha}{A} \right)^{k-1} \frac{1 - (A\alpha)^{-k}}{1 - (A\alpha)^{-1}} \right) \\
&= \frac{1}{K^2} \left(\frac{A^{2k} - 1}{A^2 - 1} + 2 \frac{\alpha}{A - \alpha} \frac{A^{2k} - 1}{A^2 - 1} - 2 \frac{\alpha}{A - \alpha} \frac{\alpha^k A^k - 1}{A\alpha - 1} \right)
\end{aligned} \tag{17}$$

We also need to compute:

$$\begin{aligned}
&\operatorname{cov}\left(\varepsilon_K, \sum_{i=0}^{k-1} A^{-i} \eta_{i+K+1} \right) = \sum_{i=0}^{k-1} A^{-i} \operatorname{cov}(\varepsilon_K, \eta_{i+K+1}) \\
&\sum_{i=0}^{k-1} A^{-i} \operatorname{cov}\left(\frac{1}{K} \sum_{j=1}^{K} \eta_j, \eta_{i+K+1} \right) = \sum_{i=0}^{k-1} A^{-i} \sum_{j=1}^{K} \frac{\alpha^{i+K+1-j}}{K} = \sum_{i=0}^{k-1} A^{-i} \sum_{j=1}^{K} \frac{\alpha^{i+j}}{K} \\
&= \frac{1}{K} \sum_{i=0}^{k-1} \left(\frac{\alpha}{A} \right)^i \alpha \sum_{j=1}^{K} \alpha^{j-1} = \frac{\alpha}{K} \left(\frac{1 - \left(\frac{\alpha}{A} \right)^k}{1 - \left(\frac{\alpha}{A} \right)} \right) \left(\frac{1 - \alpha^K}{1 - \alpha} \right)
\end{aligned} \tag{18}$$

As a consequence we have:

$$\begin{aligned}\operatorname{cov}(v_k) &= \operatorname{cov}\left(A^k\varepsilon_K + \frac{1}{K}\sum_{i=0}^{k-1}A^i\eta_{i+K+1}\right)\\ &= A^{2k}\left(\frac{1+\alpha}{K(1-\alpha)} - \frac{2\alpha}{K^2(1-\alpha)^2}\left(1-\alpha^K\right)\right) + \frac{\alpha A^{2k-1}}{K^2}\left(\frac{1-\left(\frac{\alpha}{A}\right)^k}{1-\frac{\alpha}{A}}\right)\left(\frac{1-\alpha^K}{1-\alpha}\right) + \\ &\frac{1}{K^2}\left(\frac{1-A^{2k}}{1-A^2} + \frac{2}{1-\left(\frac{A}{\alpha}\right)}\left(\frac{1-(\alpha A)^k}{1-\alpha A} - \frac{1-A^{2k}}{1-A^2}\right)\right)\end{aligned} \tag{19}$$

Figure 1 shows these curves for K = 100 and α=0.57.

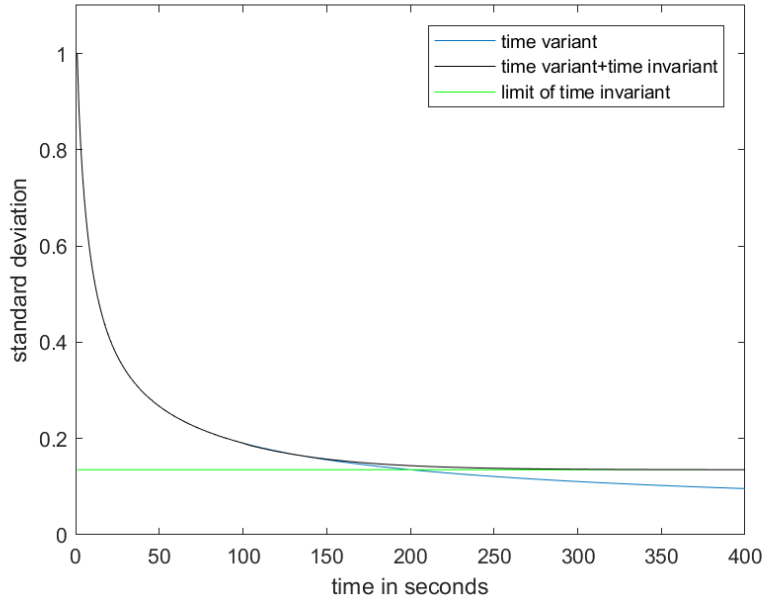

Figure 1. Error convergence curves assuming a first order model for the code multipath

Formulas for A_{MP} and A_{noise}:

For simplicity, we only use the shaping function derived from the time varying section (this is a conservative step), that is we define:

$$\varphi_\alpha(k) = \frac{\operatorname{cov}(\varepsilon_k)}{\operatorname{cov}(\varepsilon_{360})} \text{ for } k \le 360$$

$$\varphi_\alpha(k) = 1 \text{ for } k > 360 \tag{20}$$

For A_{MP}, we find the parameter α_1 such that $\varphi_{\alpha_1}(1) = 100$, which is 0.57. For A_{noise} we find the parameter α_2 such that $\varphi_{\alpha_2}(1) = 200$, which is 0.28. The final curve is then given by:

$$\sigma_{air}(k) = \sqrt{\frac{f_{L1}^4 + f_{L5}^4}{\left(f_{L1}^2 - f_{L5}^2\right)^2}} \sqrt{\varphi_{\alpha_1}(k)\left(\sigma_{MP\&AGVD,i}\right)^2 + \varphi_{\alpha_2}(k)\left(\sigma_{noise,i}\right)^2} \quad (21)$$

COMPARISON TO ACTUAL ERROR DISTRIBUTIONS

For this evaluation, we used 150 h of GNSS data collected in flight by a multi-constellation, multi-frequency receiver (Trimble BX935-INS) that tracks all the current GNSS constellations, satellites, and civil signals; in particular GPS, (L1 C/A, L1C, L2 (semi-codeless), L2C, and L5) and Galileo (E1 and E5a-E5b). This receiver is installed in a Global 5000 jet owned and operated by the William J. Hughes FAA Technical Center. The purpose of this evaluation is to see whether the model developed above describes the measurements correctly.

Code multipath estimate

The true code multipath was estimated as described in [3] using carrier leveling with cycle slip free tracks (or at least without detected cycle slips) longer than 600 s. This approach will cause the estimate to also include antenna group delays for part of the data, which is desirable, since we also need to bound them. We cannot however claim that the group delays will be included in all the estimates, because the data includes long straight and level flights, where we expect the antenna group delays to vary too slowly compared to the length of the arcs used for carrier leveling.

For the dual frequency combination code multipath, we used the ionospheric delay free combinations, and or the single frequency, we used a biased estimate of the ionospheric delay using the carrier from a second frequency. Figure 2 shows the result for one track. As expected, we observe that the code multipath in the dual frequency iono-free combination is significantly higher than in the single frequency case.

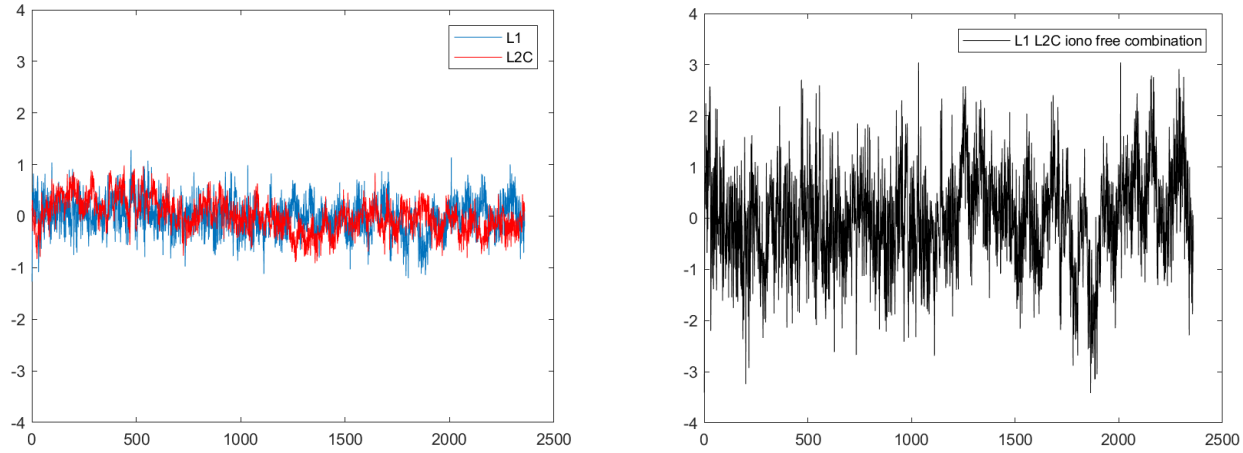

Figure 2 a) and b). Carrier leveling result for one track for L1, L2C and L1-L2C combinations.

Smoothed code multipath sample distribution

For a given satellite, time, and smoothing time k, the smoothed code multipath was obtained by applying the smoothing process coefficients to the estimated code multipath. Since the error model is a multiple of the value at convergence, we normalize each of the samples by the expression in Equation (1). At the end of this process, we obtain a sample distribution of the normalized smoothed code multipath. If this sample distribution was exactly a zero mean normal distribution, and we assumed that the error model has the dependence expressed in Equation (1), it would mean that the data matches exactly the model. In this case, A(k) would be given by the standard deviation of the sample distribution.

Overbounding the normalized sample distributions

In reality, the set of sample distributions (parametrized by k) is not Gaussian. Figure 3 shows the quantile-quantile plot of the sample distribution corresponding to k=1 (no smoothing) for GPS L1. This figure shows the sample quantiles as a function of the quantiles corresponding to a zero mean gaussian distribution. For our purposes, it is sufficient that A(k) represents the sigma of an overbounding distribution. There are several ways of computing Gaussian overbounding distributions. In this paper we use the two-step method described in [4], as it results in overbounding distributions that are stable through convolution, like in paired Gaussian overbounding, and it produces overbounding distributions with biases close to the original sample distribution. In this case, the sigma overbound was 0.35.

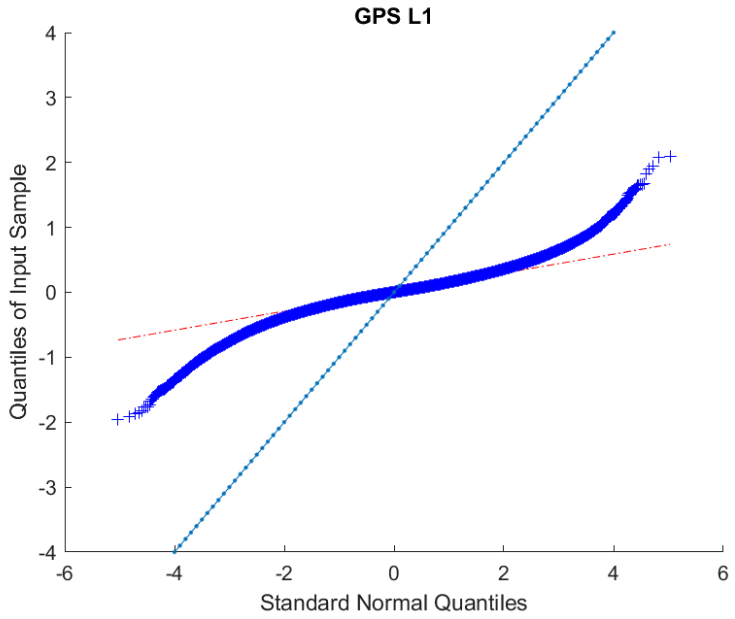

Figure 3. Q-Q plot of the sample distribution with no smoothing assuming the inflation factors at t = 0.

Empirical convergence curve and comparison to model

The process described above was performed for all smoothing times between zero and 360 s every 5 s. Figure 4 shows the resulting empirical convergence curves for GPS L1-L5, GPS L1, GPs L5, Galileo E1-E5a, Galileo E1, and Galileo E5a in blue. In the same plots, we also plot:

- the model developed in the first section (red).
- a scaled version of the model so that the value at convergence is an overbound of the empirical curve (black) at convergence

- a fitted curve where we match the converged value and adjust the parameter α so that the curve matches the measured curve at k=0.

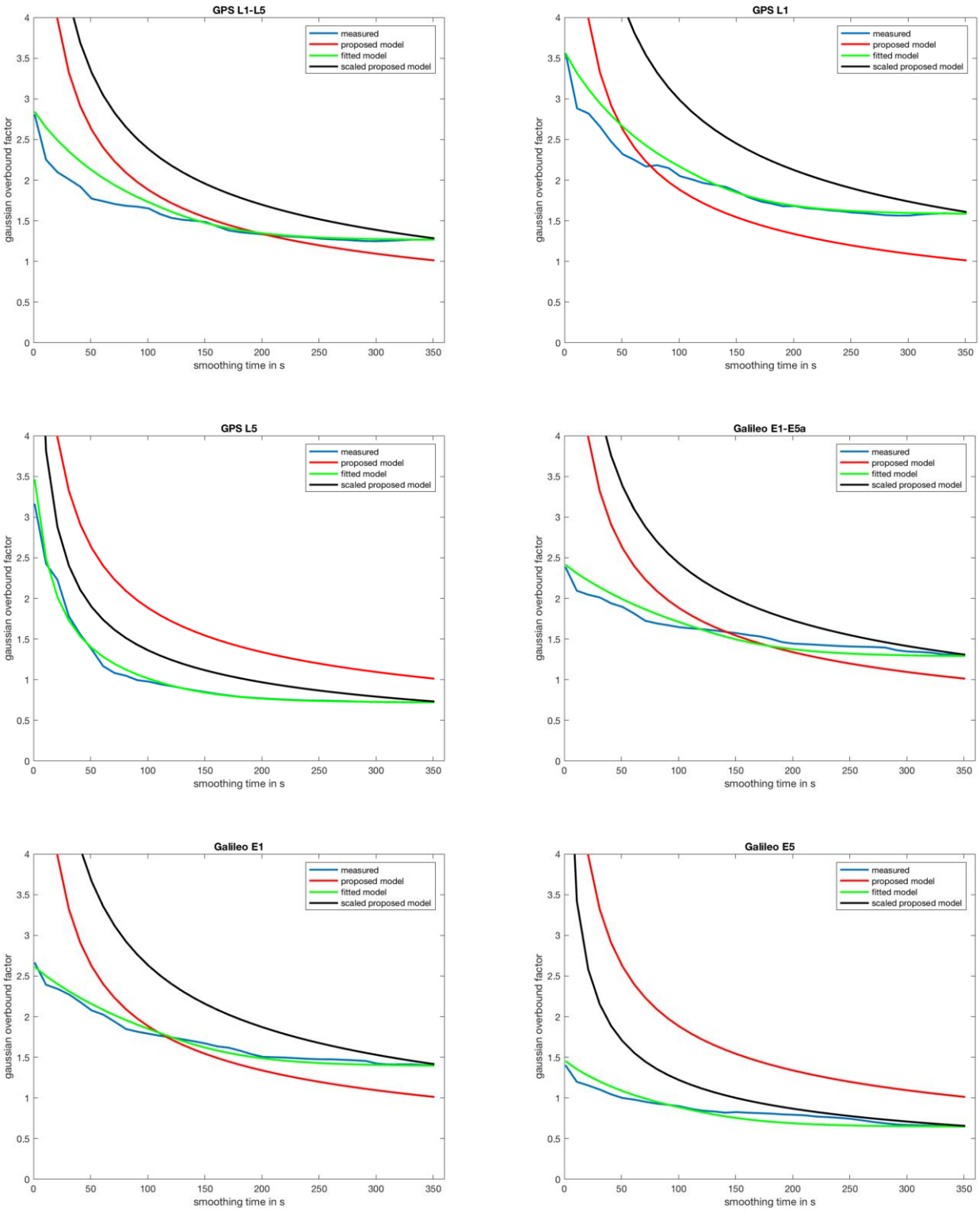

Figure 4. Empirical overbounding convergence curves (blue), model (blue), scaled model (black), fitted model (green).

We observe that for GPS L1-L5, GPS L1, Galileo E1-E5a, and Galileo E1, the model does not bound the error at convergence (which was one of the assumptions when developing the model). This does not mean that the model at convergence is incorrect, since the antenna used in the data collection was not compliant with aviation standards for example. In all cases the fitted curves match very well with the observed data (in some cases surprisingly well), which indicates that the shape of the convergence curve is adequate.

SUMMARY

Multipath and noise error bounds are derived as a function of smoothing time assuming a first order model for the code multipath and the receiver noise. These are evaluated using GPS and Galileo measurements collected in flight. The model appears to account well for the effect of smoothing for GPS and Galileo measurements collected in flight. However, in the data that we analyzed, the value at convergence is not sufficiently conservative.

ACKNOWLEDGEMENTS

This work was funded by the Federal Aviation Administration. We would also like to thank Mike Gehringer and Bill Wanner at the FAA Technical Center (for making the data collection possible), and Stuart Riley at Trimble Navigation (for lending us the receiver and for his help in processing the data).

REFERENCES

[1] WAAS Minimum Operational Performance Specification (MOPS), RTCA document DO-229E.

[2] SBAS Dual Frequency Multi-constellation Minimum Operational Standards Draft v0.6.1 June 2018.

[3] Phelts, R. Eric, Blanch, Juan, Gunning, Kazuma, Walter, Todd, and Enge, Per. “Effect of Aircraft Banking on ARAIM Performance” Proceedings of the 31st International Technical Meeting of The Satellite Division of the Institute of Navigation (ION GNSS+ 2018), Miami, Florida, September 2018.

[4] Blanch J., Walter, T., and Enge, P., "Gaussian Bounds of Sample Distributions for Integrity Analysis", Accepted for publication in *IEEE Transactions on Aerospace and Electronic Systems.*

[5] Circiu, Mihaela-Simona, Caizzone, Stefano, Felux, Michael, Enneking, Christoph, Meurer, Michael, "Improved Airborne Multipath Modelling," *Proceedings of the 31st International Technical Meeting of The Satellite Division of the Institute of Navigation (ION GNSS+ 2018)*, Miami, Florida, September 2018, pp. 2195-2209.